



Fermi National Accelerator Laboratory

FERMILAB-Pub-93/081-E

E769

## $D^{*\pm}$ Production in 250 GeV $\pi^\pm$ N Interactions

G.A. Alves et al  
the E769 Collaboration

*Fermi National Accelerator Laboratory  
P.O. Box 500, Batavia, Illinois 60510*

April 1993

Submitted to *Physical Review Letters*

## **Disclaimer**

*This report was prepared as an account of work sponsored by an agency of the United States Government. Neither the United States Government nor any agency thereof, nor any of their employees, makes any warranty, express or implied, or assumes any legal liability or responsibility for the accuracy, completeness, or usefulness of any information, apparatus, product, or process disclosed, or represents that its use would not infringe privately owned rights. Reference herein to any specific commercial product, process, or service by trade name, trademark, manufacturer, or otherwise, does not necessarily constitute or imply its endorsement, recommendation, or favoring by the United States Government or any agency thereof. The views and opinions of authors expressed herein do not necessarily state or reflect those of the United States Government or any agency thereof.*

# $D^{*\pm}$ Production in 250 GeV $\pi^\pm N$ Interactions

G.A. Alves,<sup>(1)</sup> S. Amato,<sup>(1),(a)</sup> J.C. Anjos,<sup>(1)</sup> J.A. Appel,<sup>(2)</sup>  
J. Astorga,<sup>(5)</sup> S.B. Bracker,<sup>(4)</sup> L.M. Cremaldi,<sup>(3)</sup>  
C.L. Darling,<sup>(7)</sup> R.L. Dixon,<sup>(2)</sup> D. Errede,<sup>(6),(b)</sup>  
H.C. Fenker,<sup>(2),(c)</sup> C. Gay,<sup>(4),(d)</sup> D.R. Green,<sup>(2)</sup>  
A.M. Halling,<sup>(2)</sup> R. Jedicke,<sup>(4)</sup> P.E. Karchin,<sup>(7)</sup> S. Kwan,<sup>(2)</sup>  
L.H. Lueking,<sup>(2)</sup> P.M. Mantsch,<sup>(2)</sup>  
J.R.T. de Mello Neto,<sup>(1),(e)</sup> J. Metheny,<sup>(5)</sup> R.H. Milburn,<sup>(5)</sup>  
J.M. de Miranda,<sup>(1),(a)</sup> H. da Motta Filho,<sup>(1)</sup> A. Napier,<sup>(5)</sup>  
D. Passmore,<sup>(5)</sup> A. Rafatian,<sup>(3)</sup> A.C. dos Reis,<sup>(1)</sup>  
W.R. Ross,<sup>(7),(f)</sup> A.F.S. Santoro,<sup>(1)</sup> M. Sheaff,<sup>(6)</sup>  
M.H.G. Souza,<sup>(1)</sup> W.J. Spalding,<sup>(2)</sup> C. Stoughton,<sup>(2)</sup>  
M.E. Streetman,<sup>(2)</sup> D.J. Summers,<sup>(3)</sup> S.F. Takach,<sup>(7)</sup>  
A. Wallace,<sup>(7)</sup> Z. Wu<sup>(7)</sup>

## *The Fermilab E769 Collaboration*

<sup>(1)</sup>*Centro Brasileiro de Pesquisas Físicas, Rio de Janeiro, Brazil*

<sup>(2)</sup>*Fermi National Accelerator Laboratory, Batavia, Illinois 60510*

<sup>(3)</sup>*University of Mississippi, Oxford, Mississippi 38677*

<sup>(4)</sup>*University of Toronto, Toronto, Ontario, Canada, M5S 1A7*

<sup>(5)</sup>*Tufts University, Medford, Massachusetts 02155*

<sup>(6)</sup>*University of Wisconsin, Madison, Wisconsin 53706*

<sup>(7)</sup>*Yale University, New Haven, Connecticut 06511*

(Received April 8, 1993)

We report results from Fermilab experiment E769 on the differential cross sections of  $D^{*\pm}$  charm vector mesons with respect to Feynman- $x$  ( $x_F$ ) and transverse momentum ( $P_T$ ), and on the atomic mass dependence of the production. The charm particles were produced by 250 GeV  $\pi^-$  and  $\pi^+$  beams on a target consisting of Be, Al, Cu and W foils. In the range  $0.1 < x_F < 0.6$ , the  $d\sigma/dx_F$  distribution is well fit to the form  $(1 - x_F)^n$  with  $n = 3.5 \pm 0.3 \pm 0.1$ . In the range  $P_T^2 < 4 \text{ GeV}^2$ , the  $d\sigma/dP_T^2$  distribution is well fit by the form  $\exp(-b \times P_T^2)$  with  $b = 0.70 \pm 0.07 \pm 0.04 \text{ GeV}^{-2}$ . The cross section A-dependence is parameterized by the form  $A^\alpha$  with  $\alpha = 1.00 \pm 0.07 \pm 0.02$ . These results are compared to the equivalent parameters for the inclusive production of the pseudoscalar  $D^0$  and  $D^\pm$  charm mesons, and for  $D^0$  mesons resulting from  $D^*$  decays.

PACS numbers: 12.38.Qk, 13.85.Ni, 25.80.Ls

To date, almost all measurements of the differential cross sections for charm meson production have been made using samples of pseudoscalar  $D$  mesons. Very few results using samples of vector  $D^*$  mesons have appeared in the literature [1–3], and these have been of rather limited statistics. The differential cross sections for charm production have been predicted using perturbative QCD up to next-to-leading order (NLO) [4]. These distributions depend on the quark and gluon structure functions in the beam particles and target nucleons, on the fundamental parton interactions, and on the hadronization or fragmentation of the produced charm quark. Whereas the first two components are common to the production of pseudoscalar and vector charm particles, the hadronization process can differ. We have reported our results for the  $\pi^-$  induced differential cross sections of charged and neutral  $D$  mesons [5]. The meson  $x_F$  distribution was found to be consistent with the theoretical distribution from NLO calculations for the produced quark prior to hadronization, indicating that fragmentation in this hadronic environment does not lead to a more central  $x_F$  distribution. In this report we compare our results for a high statistics  $D^*$  sample with those in [5].

In addition, the study of the  $D^*$  differential cross sections allows an examination of “leading particle” effects. (A leading charm particle shares a valence quark flavor with the beam particle.) In  $D^{*+}$  production, as in  $D^+$  production, the leading or non-leading character of the charm particle is unambiguous. (The inclusion of charge conjugate states is implied unless specifically stated otherwise.) This is not the case for  $D^0$  mesons, since they change their leading/non-leading character depending on whether they are directly produced or result from the decays of charged  $D^*$ 's. While an earlier experiment reported a large difference in the  $x_F$  distribution for leading versus non-leading  $D$  meson production [6], others have found no significant difference. The QCD calculations do not predict significant asymmetries at the parton

level (although the higher order terms do give rise to a very small asymmetry at high  $x_F$ ). Any sizeable effect would necessitate explanation in terms of either additional production mechanisms or the influence of the hadronic environment upon fragmentation [7].

Fermilab E769 is a high statistics study of charm hadroproduction by 250 GeV  $\pi^\pm$ ,  $K^\pm$  and  $p$  beams. All data were collected during the 1987-88 fixed target run using the Tagged Photon Spectrometer at Fermilab [5]. The  $D^*$  sample used in this report comes from the combined  $\pi^-$  and  $\pi^+$  data and contains three decay modes:

$$D^{*+} \rightarrow D^0\pi^+, D^0 \rightarrow K^-\pi^+ \quad (1)$$

$$D^{*+} \rightarrow D^0\pi^+, D^0 \rightarrow K^-\pi^+\pi^-\pi^+ \quad (2)$$

$$D^{*+} \rightarrow D^0\pi^+, D^0 \rightarrow K^-\pi^+\pi^0 \quad (3)$$

The use of a segmented foil target of Be, Al, Cu, and W allowed us to measure the A-dependence for  $D^*$  meson production. This can be compared to our published results on the A-dependence for pseudoscalar  $D$  meson production [8].

Employing a trigger using the transverse energy of the events measured by the calorimeter, and a high rate microprocessor-based data acquisition system, the experiment collected about 400 million events, of which about 240 million were due to pion interactions.

After full reconstruction, events are selected with two or more vertices, separated in the beam direction by a significance of at least 6 standard deviations ( $6\sigma$ ). This reduces the sample size by a factor of 14. Further analysis cuts are applied to select candidates for each  $D^0$  decay mode. The analyses for modes (1) and (2) use similar sets of cuts, with a significance of  $7\sigma$  for the vertex separation in the beam direction between the primary vertex (taken as the vertex with the highest multiplicity of tracks) and the candidate  $D^0$  decay vertex. The distance between the line of flight of

the reconstructed  $D^0$  and the primary vertex is required to be less than 90 (80)  $\mu m$  for mode (1) ((2)). For each decay track, the impact parameter measured from the secondary vertex is divided by that measured from the primary; the product of these ratios is selected to be less than 0.1 (0.01). Additionally for mode (1) the summed  $P_T^2$  of the decay tracks, with the  $P_T$  measured relative to the direction of the parent, is required to be  $> 0.4 \text{ GeV}^2$ .

For mode (3) the  $\pi^0$  is not reconstructed. Using the high precision measurement of the  $D^0$  direction (the line connecting the primary to the  $K\pi$  vertex) we solve for the  $\pi^0$  momentum vector squared. Because of the finite vertex resolution, this positive definite quantity can acquire a non-physical, negative value. In this case the position of the secondary vertex is allowed to move by one sigma in x and y (transverse to the beam direction) and another attempt at calculating the  $\pi^0$  momentum is made. This procedure is tested on a background sample using wrong charge combinations to ensure that no bias is introduced. In cases with two physical solutions, the one which gives the lower mass is used, as indicated by Monte Carlo events. The significance of the vertex separation is required to be greater than  $6\sigma$  and less than a value corresponding to 3  $D^0$  lifetimes. The largest component of decay mode (3) is  $D^0 \rightarrow K^- \rho^+, \rho^+ \rightarrow \pi^+ \pi^0$ , where the decay angular distribution is expected to have the form  $\cos^2 \theta$  ( $\theta$  is the angle between the  $D^0$  and  $\pi^0$  directions in the rest frame of the  $\rho$ .) In order to reduce background, while maintaining good efficiency for this mode, we require  $\cos \theta > 0.5$ , and the  $\pi\pi^0$  mass to be less than 1 GeV.

The Cerenkov counters are used for particle identification for all three modes. For more detailed descriptions of the cuts, refer to [9].

$D^*$  candidates are formed by combining each pion track from the primary vertex with the  $D^0$  candidate. For mode (1) ((2)) the mass difference between  $D^0\pi$  and  $D^0$  is required to be within  $\pm 2.0$  (2.5) MeV of the central value, 145.4 MeV. The

mass of the  $D^*$  candidate is plotted, and fitted using the binned maximum likelihood method, with a gaussian signal shape having rms width determined from the Monte Carlo simulation, and a linear background (Fig. 1). For mode (3) we plot  $\Delta = M(D^*) - M(D^0) - .1454$  GeV and fit it to a gaussian signal with rms width set to the Monte Carlo value and with a background parameterized in the form  $|\Delta - \delta|^\epsilon$ . The values of the parameters,  $\delta = -0.008$  and  $\epsilon = 0.5$ , are determined by fitting the distribution of the wrong charge combination. The resultant signals are  $243 \pm 18$   $(K\pi)\pi$ ,  $129 \pm 15$   $(K3\pi)\pi$  and  $147 \pm 15$   $(K\pi\pi^0)\pi$ , giving a total  $D^*$  signal size of  $519 \pm 28$ .

The acceptance is calculated using a complete Monte Carlo simulation including the effects of the detector geometry and component efficiencies, trigger and reconstruction efficiencies, and all analysis cuts. The event generator uses a leading order QCD calculation for the charm quark pair, and JETSET v6.3 [10] is used to simulate the hadronization process. The  $x_F$  and  $P_T$  dependences of the acceptance are shown for mode (1) in Fig. 2.

For each mode the mass plot is fitted in each  $x_F$  or  $P_T^2$  bin and the resultant signal corrected for acceptance. The distributions of the acceptance-corrected signals are fitted with the functional forms of  $(1 - x_F)^n$  and  $\exp(-b \times P_T^2)$  using the least-squares method. The results for the three modes are then combined to determine the best measurement of  $n$  and  $b$ . We exclude the 0.0 to 0.1 bin in the fits to the  $x_F$  distributions in order to compare our results to those for pseudoscalar mesons [5]. The results are displayed in Fig. 3, superimposed on the combined data for the three modes using a weighted average in each bin. The systematic errors in the measurement of  $n$  and  $b$  are estimated by studying the uncertainty in the acceptance corrections for the trigger, particle identification, and analysis cuts. An additional systematic error for mode (3), due to uncertainty in the shape of the background in

the mass distribution, is studied using different values of the parameter for the shape. All the systematic effects are found to be small compared to the statistical errors. The final results for the combined sample are  $n = 3.5 \pm 0.3 \pm 0.1$  for  $0.1 < x_F < 0.6$ , and  $b = 0.70 \pm 0.07 \pm 0.04 \text{ GeV}^{-2}$  for  $P_T^2 < 4 \text{ GeV}^2$ .

The values of  $n$  and  $b$  for the leading (L), and non-leading (NL) charm particles are listed in Table 1, along with the E769 results for the pseudoscalar  $D$  mesons [5] and those for the daughter  $D^0$  mesons from the  $D^*$  decays in the present analysis. The values of  $n$  for the vector particles are consistent with those for the pseudoscalars. For  $D^*$  production we measure the difference in  $n$  values,  $n_{NL}(D^*) - n_L(D^*) = 1.2 \pm 0.7$ , compared to  $1.1 \pm 0.7$  for  $D^+$  production, indicative of a weak leading particle effect. The values of  $b$  are lower for vector particle production than for the pseudoscalars, with the daughter  $D^0$  values tending to lie between the two. Table 2 includes results from other experiments on  $D^*$  production with a pion beam [1-3]. Our central values for  $b$  are lower than these measurements, although consistent.

To further investigate the question of leading production, we measured the asymmetry for (L) versus (NL)  $D^*$ 's, defined as  $A(D_L^*, D_{NL}^*) = [\sigma(D_L^*) - \sigma(D_{NL}^*)] / [\sigma(D_L^*) + \sigma(D_{NL}^*)]$ , where  $\sigma(X)$  is the number of events with meson  $X$  divided by the acceptance for  $x_F > 0$ . The result for  $D^*$  production is  $0.09 \pm 0.06$ , while for  $D^+$  production we found  $0.18 \pm 0.06$  for the equivalent asymmetry.

Using the analysis method of [8] we measure the cross section dependence on atomic mass of the target material for  $D^*$  production. Parameterizing this dependence by the form  $A^\alpha$  we find  $\alpha = 1.00 \pm 0.07 \pm 0.02$ . Of our total  $D^*$  sample, 35% is common with the sample of pseudoscalar mesons in [8], where we found  $\alpha = 1.00 \pm 0.05 \pm 0.02$ .

This research was supported by the U.S. Department of Energy, the U.S. National Science Foundation, the Brazilian Conselho Nacional de Desenvolvimento Científico e Tecnológico, and the National Research Council of Canada.

## REFERENCES

- <sup>a</sup> Now at Pontifícia Univ. Católica do Rio de Janeiro, RJ, Brazil.
- <sup>b</sup> Now at Univ. of Illinois, Urbana, IL 61801.
- <sup>c</sup> Now at SSC Laboratory, Dallas, TX 75237.
- <sup>d</sup> Now at CERN, CH-1211, Genève 23, Switzerland.
- <sup>e</sup> Now at Univ. do Estado do Rio de Janeiro, RJ, Brazil.
- <sup>f</sup> Now at Univ. of Oklahoma, Norman, OK 73071.
- [1] NA27 LEBC-EHS Collab., M. Aguilar-Benitez *et al.*, Phys. Lett. **169B**, 106 (1986).
- [2] NA32 ACCMOR Collab., S. Barlag *et al.*, Z. Phys. **39C**, 451 (1988).
- [3] NA32 ACCMOR Collab., S. Barlag *et al.*, Z. Phys. **49C**, 555 (1991).
- [4] P. Nason, S. Dawson, R.K. Ellis, Nucl. Phys. **B327**, 49 (1989).
- [5] G.A. Alves *et al.*, Phys. Rev. Lett. **69**, 3147 (1992).
- [6] NA27 LEBC-EHS Collab., M. Aguilar-Benitez *et al.*, Phys. Lett. **161B**, 400 (1985).
- [7] R. Vogt, S.J. Brodsky, P. Hoyer, Nucl. Phys. **B383**, 643 (1992);  
M.L. Mangano, P. Nason, G. Ridolfi, Univ. of Pisa: IFUP-TH-37/92.
- [8] G.A. Alves *et al.*, Phys. Rev. Lett. **70**, 722 (1993).

- [9] S. Amato, Ph.D. thesis, Centro Brasileiro de Pesquisas Físicas, 1992 (unpublished);  
J.M. de Miranda, Ph.D. thesis, Centro Brasileiro de Pesquisas Físicas, 1992 (unpublished);  
A. Rafatian, Ph.D. thesis, Univ. of Mississippi, 1993 (in preparation).
- [10] B. Nilsson-Almqvist and E. Stenlund, *Comput. Phys. Commun.* **43**, 387 (1987).

TABLES

TABLE I. Production parameters for E769 with 250 GeV  $\pi$  incident on Be, Al, Cu, and W targets (statistical errors only.)  $L$  and  $NL$  labels for the daughter values refer to the leading and non-leading  $D^*$  parent meson.

	$D^*$	$D^0(\text{daughter})$	$D^+$ [5]	$D^0$ [5]
#events	$519 \pm 28$	$519 \pm 28$	$700 \pm 34$	$607 \pm 41$
$x_F$ fit range	0.1 to 0.6	0.1 to 0.6	0.1 to 0.7	0.1 to 0.7
$n$	$3.5 \pm 0.3$	$3.8 \pm 0.3$	$3.7 \pm 0.3$	$4.2 \pm 0.5$
$n_L$	$2.9 \pm 0.4$	$3.0 \pm 0.4$	$3.3 \pm 0.5$	
$n_{NL}$	$4.1 \pm 0.5$	$5.2 \pm 0.7$	$4.4 \pm 0.5$	
$P_T^2$ fit range ( $\text{GeV}^2$ )	0 to 4	0 to 4	0 to 4	0 to 4
$b$ ( $\text{GeV}^{-2}$ )	$0.70 \pm 0.07$	$0.87 \pm 0.07$	$0.99 \pm 0.06$	$1.08 \pm 0.08$
$b_L$	$0.58 \pm 0.09$	$0.78 \pm 0.08$	$1.05 \pm 0.08$	
$b_{NL}$	$0.79 \pm 0.09$	$0.94 \pm 0.10$	$0.92 \pm 0.08$	

TABLE II. Comparison of  $D^*$  production parameters from experiments with incident  $\pi$  beams.

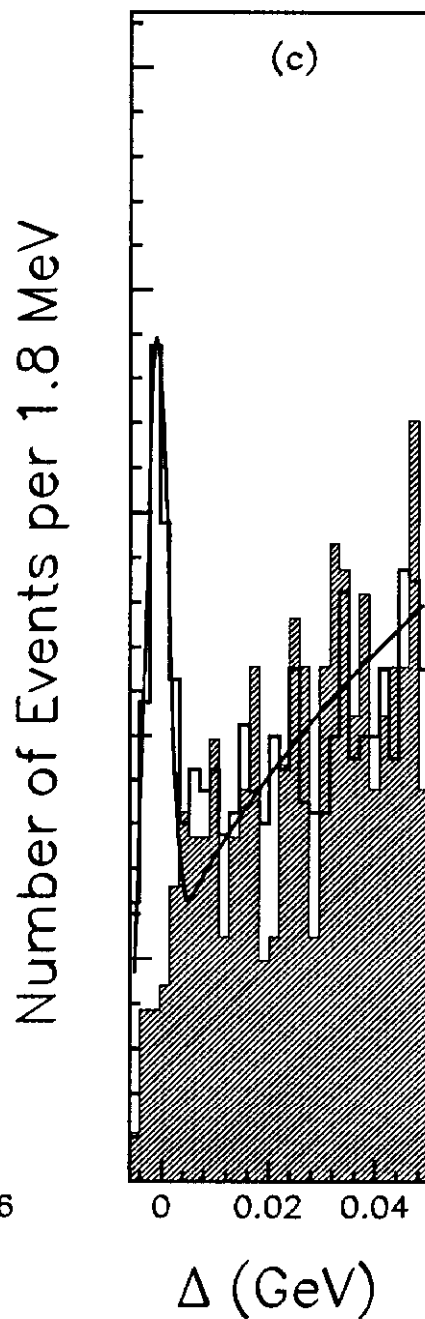
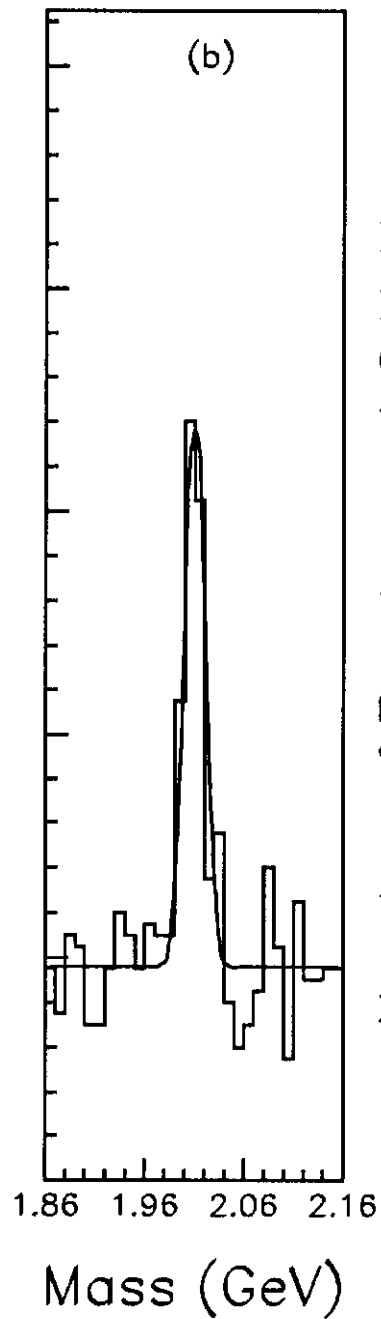
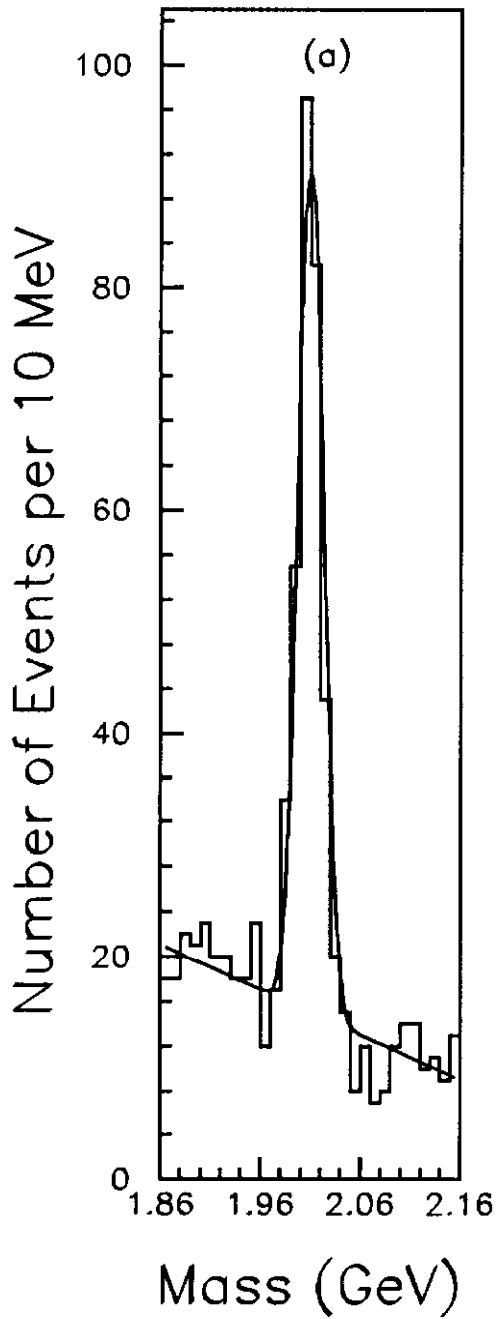
Expt.	NA27 [1]	NA32 [2]	NA32 [3]	E769
$P_{beam}$ (GeV)	360	200	230	250
Target	H	Si	Cu	Be,Al,Cu,W
#events	8.5	46	147	519
$x_F$ fit range	0.0 to 0.5	0.0 to 0.7	0.0 to 0.8	0.1 to 0.6
$n$	$4.3^{+1.8}_{-1.5}$	$2.8^{+1.1}_{-0.9}$	$3.14^{+0.40}_{-0.39}$	$3.5 \pm 0.3$
$n_L$		$4.7^{+1.9}_{-1.6}$	$2.62^{+0.53}_{-0.49}$	$2.9 \pm 0.4$
$n_{NL}$		$1.7^{+1.4}_{-1.0}$	$3.83^{+0.66}_{-0.62}$	$4.1 \pm 0.5$
$P_T^2$ fit range (GeV <sup>2</sup> )	0 to 3	0 to 5	0 to 10	0 to 4
$b$ (GeV <sup>-2</sup> )	$0.9 \pm 0.4$	$0.9^{+0.3}_{-0.2}$	$0.79 \pm 0.07$	$0.70 \pm 0.07$
$b_L$			$0.71^{+0.09}_{-0.08}$	$0.58 \pm 0.09$
$b_{NL}$			$0.90 \pm 0.11$	$0.79 \pm 0.09$

## FIGURES

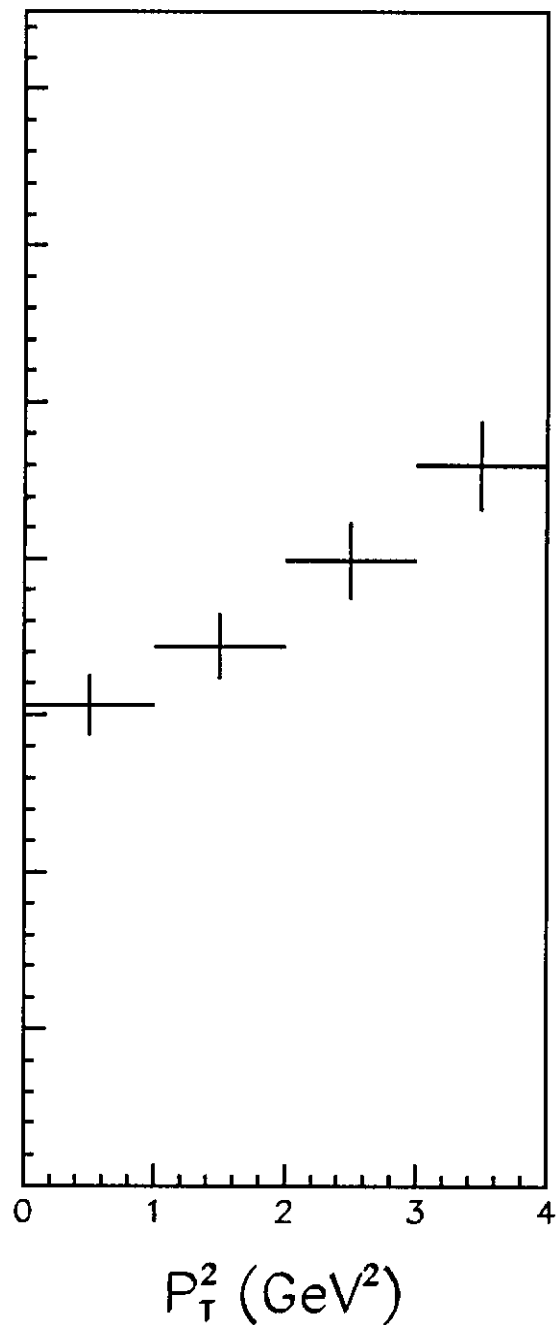
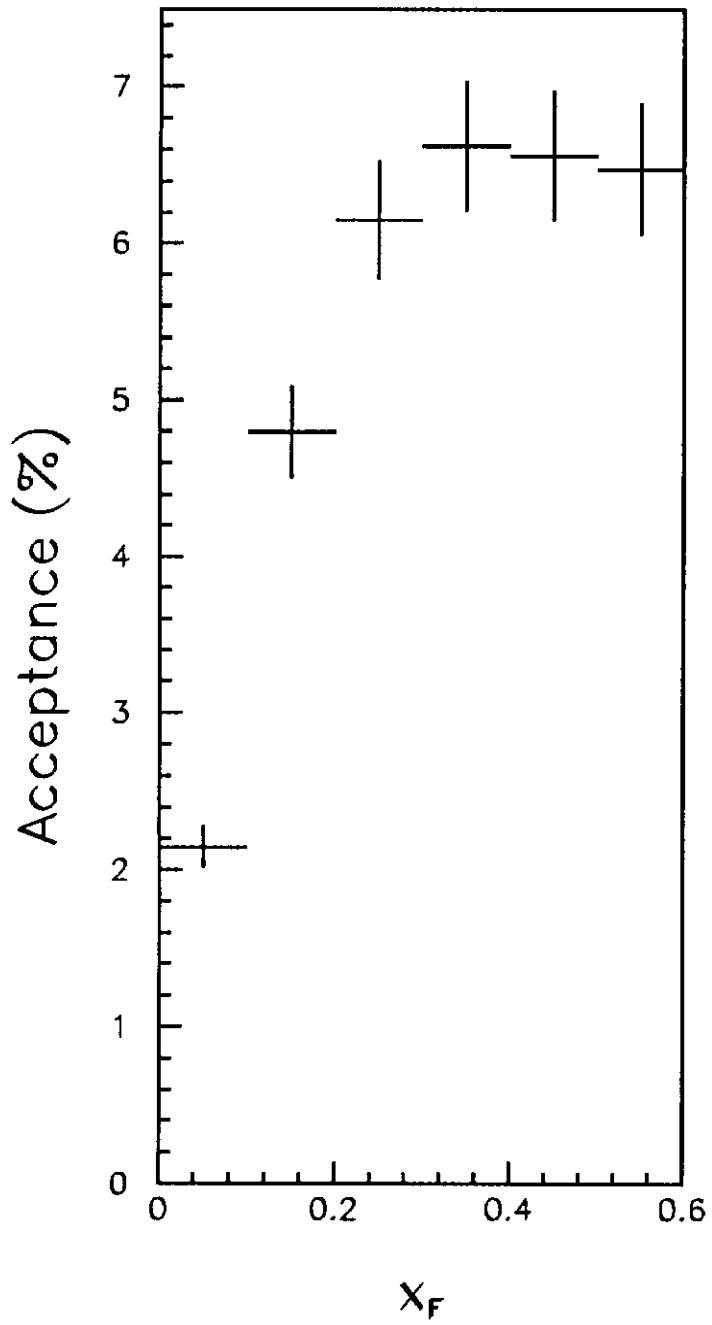
FIG. 1. Mass distributions for (a)  $D^{*+} \rightarrow D^0(K^-\pi^+)\pi^+$  and (b)  $D^{*+} \rightarrow D^0(K^-\pi^+\pi^-\pi^+)\pi^+$ , and mass difference  $\Delta$  for (c)  $D^{*+} \rightarrow D^0(K^-\pi^+\pi^0)\pi^+$ . The shaded area in c shows the distribution for the wrong charge combination, from which the background shape is determined. The fits to the data are described in the text.

FIG. 2.  $x_F$  and  $P_T^2$  acceptances for  $D^{*+} \rightarrow D^0(K^-\pi^+)\pi^+$ .

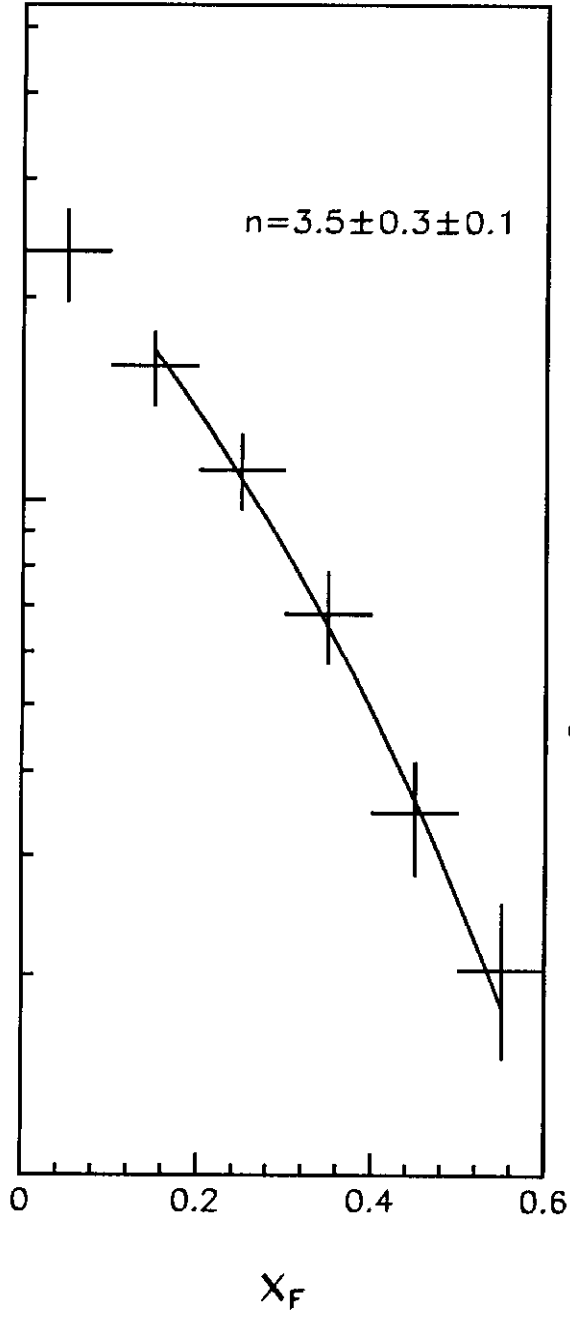
FIG. 3. Differential cross sections versus  $x_F$  and  $P_T^2$  for the combined  $D^*$  sample. The distributions are described in the text. The errors plotted are statistical only.



18



$d\sigma/dx_F$  (Arbitrary Scale)



$d\sigma/dP_T^2$  (Arbitrary Scale)

